

Photosynth Res (2006) 90:5–15
DOI 10.1007/s11120-006-9090-8

REGULAR PAPER

Optical spectroscopic studies of light-harvesting by pigment-reconstituted peridinin-chlorophyll-proteins at cryogenic temperatures

Robielyn P. Ilagan · Timothy W. Chapp ·
Roger G. Hiller · Frank P. Sharples ·
Tomáš Polívka · Harry A. Frank

Received: 4 May 2006 / Accepted: 31 July 2006 / Published online: 22 September 2006
© Springer Science+Business Media B.V. 2006

Abstract Low temperature, steady-state, optical spectroscopic methods were used to study the spectral features of peridinin-chlorophyll-protein (PCP) complexes in which recombinant apoprotein has been refolded in the presence of peridinin and either chlorophyll *a* (Chl *a*), chlorophyll *b* (Chl *b*), chlorophyll *d* (Chl *d*), 3-acetyl-chlorophyll *a* (3-acetyl-Chl *a*) or bacteriochlorophyll *a* (BChl *a*). Absorption spectra taken at 10 K provide better resolution of the spectroscopic bands than seen at room temperature and reveal specific pigment–protein interactions responsible for the positions of the Q_y bands of the chlorophylls. The study reveals that the functional groups attached to Ring I of the two protein-bound chlorophylls modulate the Q_y and Soret transition energies. Fluorescence excitation spectra were used to compute energy transfer efficiencies of the various complexes at room temperature and these were correlated with previously reported ultrafast, time-resolved optical spectroscopic dynamics data. The results illustrate the robust nature and value of the PCP complex, which maintains a high efficiency of antenna

function even in the presence of non-native chlorophyll species, as an effective tool for elucidating the molecular details of photosynthetic light-harvesting.

Keywords Absorption · Chlorophyll · Energy transfer efficiency · Fluorescence · Fluorescence excitation · Low temperature · Peridinin-chlorophyll *a*-protein · Reconstitution

Abbreviations

BChl <i>a</i>	Bacteriochlorophyll <i>a</i>
Chl	Chlorophyll
FMO	Fenna–Matthews–Olson
FWHM	Full width at half maximum
HPLC	High-performance liquid chromatography
HSPCP	High-salt peridinin-chlorophyll <i>a</i> -protein
ICT	Intramolecular charge transfer
LH1	Light-harvesting complex 1 of purple bacteria
LH2	Light-harvesting complex 2 of purple bacteria
MFPCP	Main-form peridinin-chlorophyll <i>a</i> -protein
2-MTHF	2-Methyl tetrahydrofuran
PCP	Peridinin-chlorophyll-protein

R. P. Ilagan · T. W. Chapp · H. A. Frank (✉)
Department of Chemistry, University of Connecticut, 55
North Eagleville Road, Storrs, CT 06269-3060, USA
e-mail: harry.frank@uconn.edu

R. G. Hiller · F. P. Sharples
School of Biological Sciences, Macquarie University, North
Ryde, NSW 2109, Australia

T. Polívka
Institute of Physical Biology, University of South Bohemia,
Nové Hrad, Czech Republic

Introduction

Photosynthetic organisms have bioengineered a wide variety of protein-based structures to carry out photosynthetic light-harvesting (Frigaard et al. 2004). High-resolution molecular structures of many of these systems are providing important clues into the molecular features that control light-harvesting in

photosynthesis (Germeroth et al. 1993; Hofmann et al. 1996; Hu et al. 1995; Koepke et al. 1996; Kühlbrandt et al. 1994; Law et al. 2004; Liu et al. 2004; McDermott et al. 1995; Roszak et al. 2003). To understand fully how these naturally occurring pigment–protein complexes harvest light so efficiently, it is necessary to employ spectroscopic tools that reveal directly the dynamics and efficiency of energy transfer and the nature of the excited energy states associated with the bound pigments. The spectroscopic studies are aided by the ability to make systematic alterations in the structures of the light-harvesting complexes, and then to examine how these changes manifest themselves in the spectroscopic observables, dynamics of energy transfer and efficiency of antenna function (Akahane et al. 2004; Cammarata et al. 1990; Chadwick et al. 1987; Crielgaard et al. 1994; Croce et al. 1999; Davidson and Cogdell 1981; Frank 1999; Fraser et al. 1999; Morosinotto et al. 2002; Olivera et al. 1994; Olsen et al. 1997; Plumley and Schmidt 1987; Remelli et al. 1999; Struck and Scheer 1991; Struck et al. 1992).

The peridinin-chlorophyll-protein (PCP) complex from the dinoflagellae, *Amphidinium carterae*, is an example where many of these approaches have been applied. Atomic resolution structural analysis by X-ray diffraction to 2.0 Å resolution (Hofmann et al. 1996) has been augmented by pigment reconstitutions and protein refolding studies (Miller et al. 2005; Polívka et al. 2005). Steady-state and time-resolved spectroscopy (Bautista et al. 1999a; Kleima et al. 2000a; Kleima et al. 2000b; Krueger et al. 2001; Linden et al. 2004; Shima et al. 2003; Zigmantas et al. 2002; Zimmermann et al. 2002) has been carried out on the excited singlet and triplet states associated with the bound pigments. The X-ray crystallographic analysis of PCP revealed a trimeric structure of subunits (Hofmann et al. 1996) where eight peridinin and two chlorophyll *a* (Chl *a*) molecules (Fig. 1) bind non-covalently in a roughly C_2 symmetrical arrangement in each of the three individual subunits. The peridinin are assembled in clusters of four within the subunits, surrounding, and in van der Waals contact with, one chlorophyll *a* (Chl *a*) (Fig. 1). The two Chl molecules within a subunit have a center-to-center distance of 17.4 Å. Steady-state and ultrafast optical spectroscopic investigations on peridinin in solution and on the main-form PCP (MFPCP) have explored its photoinduced excited-state processes and energy transfer pathways (Carbonera et al. 1999; Damjanovic et al. 2000; Kleima et al. 2000; Krueger et al. 2001; Ritz et al. 2000; Shima et al. 2003; Zimmermann et al. 2002). In addition, a variant form, the high-salt PCP (HSPCP), has been studied in the same manner (Ilagan et al. 2004; Sharples et al. 1996).

Adding to the arsenal of PCP complexes that can be used for structural and spectroscopic studies, Miller and coworkers (Miller et al. 2005) prepared and Polívka and coworkers (Polívka et al. 2005) studied the N-domain and full-length PCP apoproteins expressed in *Escherichia coli* and reconstituted with the total pigment extract from native PCP to produce a fully functional complex with a high peridinin-to-Chl *a* energy transfer efficiency. Also, they demonstrated that in the N-domain PCP apoprotein the bound Chl *a* molecules could be replaced by other Chls using the N-domain apoprotein incorporating the requisite stoichiometric amount of peridinin.

In this paper, we present a low temperature, steady-state, optical spectroscopic investigation of the spectral features of PCP complexes in which recombinant apoprotein has been refolded in the presence of peridinin and either chlorophyll *a* (Chl *a*), chlorophyll *b* (Chl *b*), chlorophyll *d* (Chl *d*), 3-acetyl-chlorophyll *a* (3-acetyl-Chl *a*) or bacteriochlorophyll *a* (BChl *a*). We use fluorescence excitation spectroscopy to examine in detail the peridinin-to-Chl energy transfer efficiencies of the various complexes at room temperature and

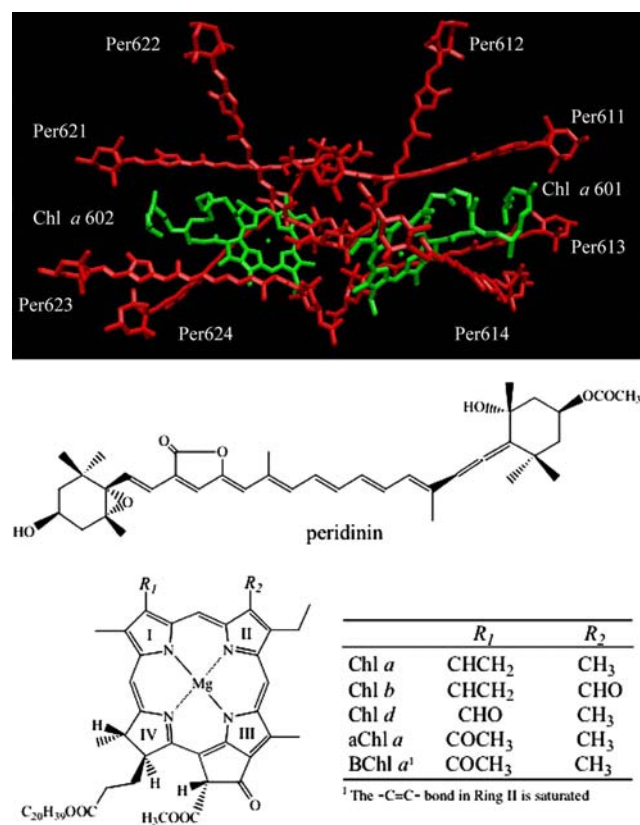


Fig. 1 Structure of the pigments in a monomeric subunit of the MFPCP complex. The coordinates were taken from Protein Data Bank with 1PPR code. Also shown are the structures of peridinin and the chlorophylls used in this study

correlate the results with previously reported ultrafast, time-resolved optical spectroscopic dynamics data (Polívka et al. 2005). The low temperature data provide better resolution of the spectroscopic bands than seen at room temperature and reveal specific pigment–protein interactions responsible for the observed Chl transition energies.

Materials and methods

Sample preparation

The PCP complexes were reconstituted from N-domain apoprotein with peridinin and either Chl *a*, Chl *b*, Chl *d*, 3-acetyl-Chl *a* or BChl *a* (Fig. 1) as described (Miller et al. 2005). Size exclusion chromatography shows the reconstituted PCP to be approximately 40 kDa in apparent molecular mass; i.e., the same as that of the native PCP, suggesting that the samples used here consist of monomeric protein structures. The purified reconstituted PCP complexes were stored at 4°C until ready for use in the spectroscopic experiments. For the cryogenic experiments, the PCP complexes were dissolved in a buffer containing 50 mM Tricine, 20 mM KCl buffer and 60% (v/v) glycerol at pH 7.6.

Chl *a* and Chl *b* were obtained from Sigma-Aldrich. Chl *d* and BChl *a* were extracted from the cyanobacterium, *Acaryochloris marina*, and the bacterium, *Rhodospirillum rubrum*, respectively. Total pigments were extracted from *A. marina* cells with 2-butanol and the extract dried in a gentle stream of nitrogen and Chl *d* was purified by HPLC as described below. BChl *a* was extracted from *R. rubrum* whole cells with 50:50 (v/v) acetone:methanol. The extracted solution was filtered, dried and redissolved in 50:50 (v/v) petroleum ether:methanol. The methanol phase, in which BChl *a* was dissolved, was collected and dried with nitrogen gas. The BChl *a* solution was subjected to an alumina column chromatography with increasing percent of acetone in hexane. 3-Acetyl-Chl *a* was obtained as an oxidation product of BChl *a* during its isolation from *R. rubrum*. All Chls were further purified using a Millipore Waters 600E HPLC system employing a Nova-Pak C₁₈ column. For Chl *a* and Chl *b*, isocratic runs of acetone:methanol:water (75:20:5, v/v/v) were used as the mobile phase with a flow rate of 0.5 mL min^{−1}. For Chl *d* and BChl *a*, the mobile phase used a combination of solvent A (acetonitrile:methanol—50:50, v/v) and solvent B (solvent A:water—50:50, v/v). The run was programmed as follows: 0–5 min, linear gradient from 80% solvent A and 20% solvent B to 99% solvent A and 1% solvent B; and, 5–30 min, isocratic 99% solvent

A and 1% solvent B with a flow rate of 1.0 mL min^{−1}. 3-acetyl-Chl *a* was separated from BChl *a* using solvent A (acetonitrile:methanol:water—87:10:3, v/v/v) and solvent B (hexane:propanol—4:1, v/v) as the mobile phase. The mobile phase was programmed as follows: 0–20 min, linear gradient from 100% solvent A to 95% solvent A and 5% solvent B; and, 20–30 min, isocratic 95% solvent A and 5% solvent B with a flow rate of 1.0 mL min^{−1}. The collected samples were dried with a gentle stream of nitrogen gas and then redissolved in 2-methyl tetrahydrofuran (2-MTHF).

Spectroscopy

Absorption spectra were taken at 10 K using a Cary 50 UV-visible spectrometer and a Janis model STVP100 helium vapor flow cryostat using 1 cm pathlength polymethacrylate cuvettes. The fluorescence and fluorescence excitation spectra of the PCP complexes were taken at 77 K using a Jobin Yvon Horiba Fluorolog-3 spectrofluorometer model FL3-22 on samples immersed in a custom built optical dewar (Kontes) as described (Ilagan et al. 2004).

Results

Absorption spectroscopy

The 10 K absorption spectra of the PCP complexes reconstituted with peridinin and either Chl *a*, Chl *b*, Chl *d*, 3-acetyl-Chl *a* or BChl *a* are shown in Fig. 2. All of the complexes exhibit strong absorption in the region 450–575 nm associated with peridinin. For the complexes reconstituted with Chl *a* and Chl *b*, a double peak is evident in the Soret region (near 450 nm), but this is not seen in complexes containing Chl *d*, 3-acetyl-Chl *a* or BChl *a*. In the long-wavelength absorption region of the spectra, the Q_y band of all the Chls is very sharp and appears at 646 nm for Chl *b*, 667 nm for Chl *a*, 682 nm for 3-acetyl-Chl *a*, 697 nm for Chl *d* and 782 nm for BChl *a*. All the Q_y bands are blue-shifted compared to the spectra taken at room temperature. Also, except for Chl *d* that exhibits a weaker shift of 59 ± 6 cm^{−1}, all are shifted by the same amount, 110 ± 15 cm^{−1}. Also, in the PCP complex containing BChl *a*, a second peak on the long-wavelength side of the primary Q_y feature is observed at 799 nm (Fig. 2) and a trace of 3-acetyl-Chl *a* can be seen in the absorption spectrum of the complex with BChl *a*.

For comparison and analysis of the Chl spectra of the complexes, absorption spectra of the isolated and purified Chls in 2-MTHF were taken at 10 K. 2-MTHF

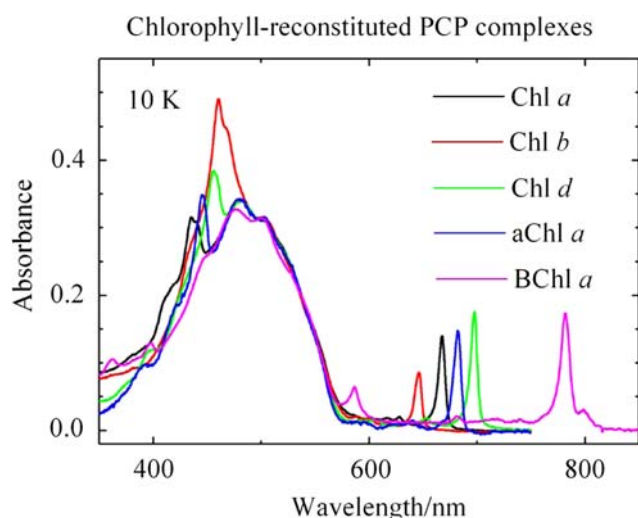


Fig. 2 Absorption spectra of the PCP complexes reconstituted with peridinin and either Chl *a*, Chl *b*, Chl *d*, aChl *a* (3-acetyl-Chl *a*) or BChl *a*. The spectra were taken at 10 K and were normalized at 500 nm

forms a clear glass at that temperature and has been used previously in this type of analysis (Ilagan et al. 2004). Figure 3 shows the 10 K absorption spectra of the Chl solutions in the Q_y region plotted on a

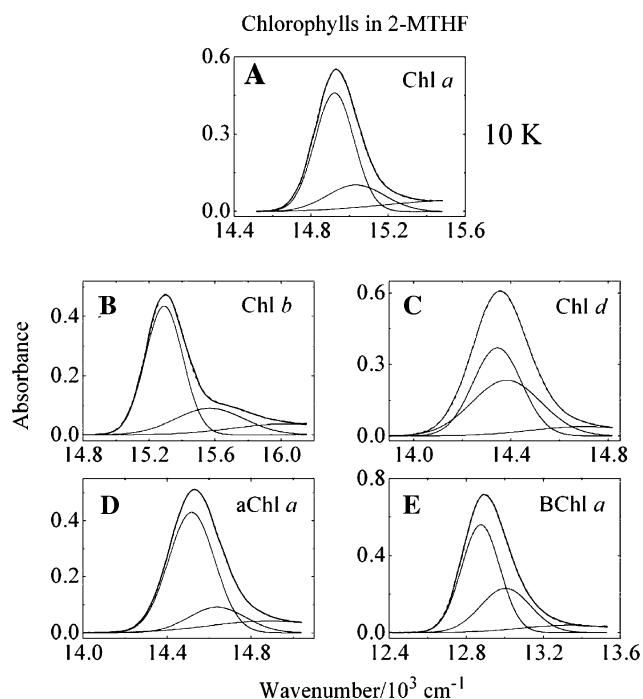


Fig. 3 Gaussian deconvolutions of the 10K absorption spectra in the Q_y region of purified Chls in 2-MTHF solvent. The fit (dashed line) is the sum of two Gaussian components built on a broad background. The data for the Gaussian deconvolution of the Chl *a* spectrum was taken from a previous study (Ilagan et al. 2004)

wavenumber scale. The spectra were analyzed by Gaussian deconvolution and were well fit using a sum of two components that were allowed to vary in amplitude, position and width built on a broad baseline. The Gaussian deconvolutions of the solution spectra were all very similar (Fig. 3) and revealed a prominent spectral origin and a broad phonon wing at higher energy. The wavelengths of the prominent peaks computed from the wavenumber fits are 670 nm for Chl *a*, 654 nm for Chl *b*, 697 nm for Chl *d*, 689 nm for 3-acetyl-Chl *a* and 777 nm for BChl *a*. The results indicate the chlorophyll–protein interaction induces a blue-shift in the case of Chl *a*, Chl *b* and 3-acetyl-Chl *a*, no shift for Chl *d* and a red-shift for BChl *a*.

Figure 4 shows the 10 K absorption spectral profiles of the reconstituted PCP complexes in the Q_y region on a wavenumber scale fitted using Gaussian functions that were also allowed to vary in amplitude, position and width. The spectra from the PCP complexes containing Chl *a*, Chl *b* and BChl *a* required four Gaussian components on a broad absorption background (Fig. 4A, B, E) for a good fit. The spectra from the complexes having Chl *d* and 3-acetyl-Chl *a* required only two Gaussian functions on a broad absorption background (Fig. 4C, D) for a good fit.

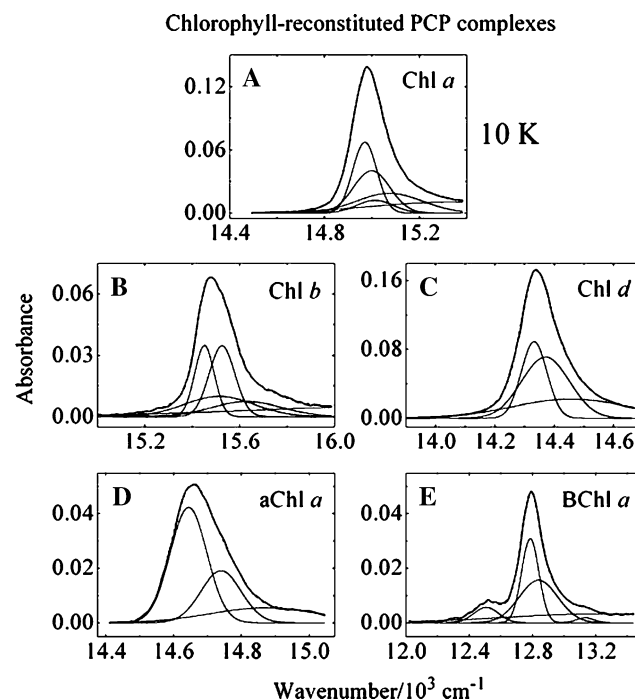


Fig. 4 Gaussian deconvolutions of the 10K absorption spectra in the Q_y region of PCP complexes reconstituted with peridinin and: (A) Chl *a*; (B) Chl *b*; (C) Chl *d*; (D) aChl *a* (3-acetyl-Chl *a*); and (E) BChl *a*

Spectral reconstruction

Linear combinations of the absorption spectra of peridinin and the various Chls taken in 2-MTHF at 10 K were used to reconstruct the spectral line shapes of the complexes in the region 375–600 nm. According to previously published procedures (Ilagan et al. 2004), individual peridinin spectra were constrained to have identical intensities, but were allowed to vary with respect to wavelength. The spectra of the individual Chls were allowed to have any intensity and wavelength. For all of the complexes, two Chl and eight peridinin spectra were used to fit the lineshapes (Fig. 5A–E). The spectra of all the complexes were best fit using two blue-shifted peridinins and three separated pairs of peridinin spectra (Fig. 5A–E), one of which needed to be significantly red-shifted to accommodate the long-wavelength region of the spectra. In the complexes containing Chl *a* and Chl *b*, the Soret bands of the two Chls are split and have noticeably different intensities. This required two separate Chl spectra to reproduce the absorption lineshapes in this region (Fig. 5A, B; Table 1). No splitting of the Soret bands was evident for the complexes with Chl *d*, 3-acetyl-Chl *a* and BChl *a*, so the spectra were able to be fit in this region

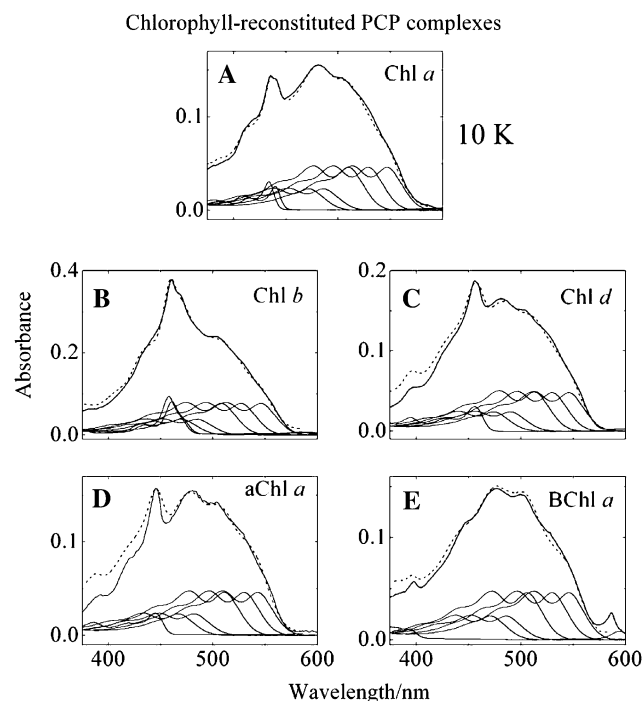


Fig. 5 Reconstruction of the 10K absorption spectra of the reconstituted PCP complexes in the 375–600 nm region. The analysis was carried out by linearly combining individual 10 K absorption spectra of peridinin and Chl taken in 2-MTHF solvent as described in the text

assuming that the two Chls were identical. A summary of the wavelengths of the spectral origins of the individual peridinins and the Chl bands assigned in this analysis is given in Table 1.

Fluorescence spectroscopy

Fluorescence spectra of the reconstituted PCP complexes at 77 K are shown in Fig. 6. The spectra display a prominent narrow band at 671 nm (full width at half maximum, FWHM = 8.5 nm) for Chl *a*, 647 nm (FWHM = 10 nm) for Chl *b*, 699 nm (FWHM = 8 nm) for Chl *d*, 686 nm (FWHM = 9.5 nm) for 3-acetyl-Chl *a* and 787 nm (FWHM = 14.5 nm) for BChl *a*. All of the spectra show structured vibronic features to the red of the main band. In the PCP complex with BChl *a*, a shoulder at 798 nm on the red side of the main peak is clearly evident.

Fluorescence excitation spectroscopy

Figure 7 shows the fluorescence excitation spectra of the complexes recorded at room temperature overlaid with their 1-*T* spectra, where *T* is transmittance. The Chl fluorescence was monitored at various wavelengths between 675 and 850 nm, and the fluorescence excitation spectra were found to be independent of the monitoring wavelength. The peridinin-to-Chl energy transfer efficiencies obtained from the spectra were averaged over the 450–515 nm wavelength range and were: $94 \pm 2\%$ (Chl *a*), $92 \pm 2\%$ (Chl *b*), $96 \pm 3\%$ (Chl *d*), $99 \pm 1\%$ (3-acetyl-Chl *a*) and $\sim 100\%$ (BChl *a*).

Discussion

Low temperature absorption spectra

The 10 K absorption spectra of the reconstituted PCP complexes (Fig. 2) show significantly higher resolution than the spectra taken at room temperature (Polívka et al. 2005). This allows a more detailed look at how changes in the structure of the incorporated Chl affect the spectral profiles. The 10 K lineshape of the PCP complex reconstituted with Chl *a* (Fig. 2) is very similar to that from the native PCP complex (Ilagan et al. 2004), the major characteristics being the splitting of the Soret band near 435 nm and the shoulder on the red side of the peridinin maximum. These features are clearly evident (Figs. 2, 5A) in both reconstituted and native complexes (Ilagan et al. 2004). This supports the notion that the structures of these two complexes are very similar.

Table 1 Spectral origins of the eight peridinin and the positions of the Soret peaks and Q_y bands of the two Chls derived from the spectral analysis of the 10 K absorption spectra of the reconstituted PCP complexes

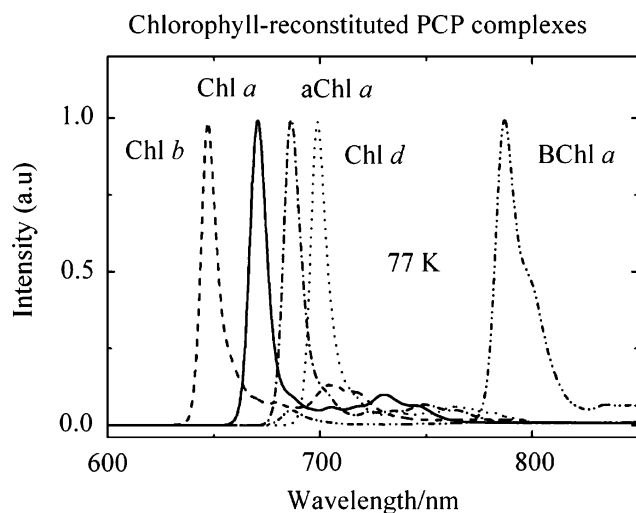
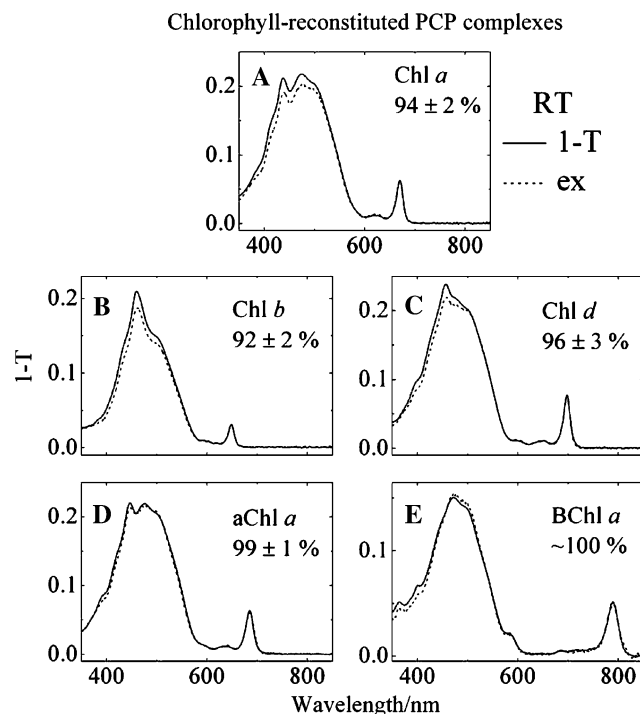
PCP complex	Peridinin								Chl		Reference	
									Soret	Q _y		
	1	2	3	4	5	6	7	8			1	2
MFPCP	470	485	522	522	526	526	544	544	434	439	665	667 (Ilagan et al. 2004)
HSPCP	na	489	533	533	533	533	533	na	436	441	667	676 (Ilagan et al. 2004)
Chl <i>a</i>	472 ± 2	486 ± 2	510 ± 1	510 ± 1	529 ± 1	529 ± 1	548 ± 1	548 ± 1	434 ± 1	440 ± 1	667	668
Chl <i>b</i>	470 ± 3	485 ± 2	508 ± 1	508 ± 1	527 ± 2	527 ± 2	546 ± 2	546 ± 2	458 ± 1	461 ± 1	644	647
Chl <i>d</i>	474 ± 2	490 ± 2	513 ± 1	513 ± 1	530 ± 1	530 ± 1	546 ± 1	546 ± 1	456 ± 2	456 ± 2	697	697
aChl <i>a</i>	467 ± 2	482 ± 2	511 ± 2	511 ± 2	530 ± 2	530 ± 2	543 ± 1	543 ± 1	446 ± 1	446 ± 1	683	683
BChl <i>a</i>	472 ± 2	486 ± 2	507 ± 2	507 ± 2	531 ± 1	531 ± 1	545 ± 1	545 ± 1	365 ± 1	365 ± 1	782	782

The numbers are in nm units and the uncertainties represent the range of values that give an acceptable fit to the data

MFPCP is main-form PCP, HSPCP is high-salt PCP, aChl *a* is 3-acetyl-Chl *a*, na is not applicable

The 10 K absorption spectra of the reconstituted PCP complexes (Fig. 2) also display blue-shifted Q_y bands compared with those spectra of the complexes taken at room temperature, and except for Chl *d* that exhibits a shift of $59 \pm 6 \text{ cm}^{-1}$, are all shifted by $110 \pm 15 \text{ cm}^{-1}$. This is opposite to the low temperature-induced red-shift observed for the 850 nm-absorbing BChl molecules in LH2 complexes from photosynthetic bacteria which was explained in terms of a structural change of the LH2 complex upon glass formation at low temperatures that increased excitonic coupling between the BChls (Wu et al. 1997). This cannot be the case for the PCP complexes here because the two Chl molecules are too far apart (17.4 Å) to be excitonically coupled. However, the blue-shift may result from a slight change in the planarity of the Chl macrocycles. Assuming that glass formation induces a

structural change (Wu et al. 1997) in the immediate environment of the Chls in the PCP complexes, one may expect a corresponding change in the conformation of the macrocycles. It has been shown that these conformational changes may induce either red- or blue-shifts of Chl Q_y bands (Gudowska-Nowak et al. 1990). The fact that the shift is very similar ($110 \pm 15 \text{ cm}^{-1}$) for all chlorophyll species except Chl *d*

**Fig. 6** Fluorescence spectra of the PCP complexes reconstituted with peridinin and either Chl *a*, Chl *b*, Chl *d*, aChl *a* (3-acetyl-Chl *a*) or BChl *a* taken at 77 K. The spectra were normalized to their λ_{max} values**Fig. 7** Overlay of the room temperature fluorescence excitation (ex) and 1-T (where T is transmittance) spectra of reconstituted PCP complexes containing: (A) Chl *a*; (B) Chl *b*; (C) Chl *d*; (D) aChl *a* (3-acetyl-Chl *a*); and (E) BChl *a*. The intensity of each fluorescence excitation spectrum was normalized to correspond to the intensity of its corresponding 1-T spectrum in the Q_y region

suggests that the structural change affects the macrocycle in the vicinity of Ring I because all the Chls except Chl *d* have a large substituent in the position *R1* (Fig. 1). Thus, if one assumes a low-temperature-induced protein structural change in the immediate environment of Ring I, this may lead to a distortion of the Chl macrocycle and consequently to the observed blue-shift. For Chl *d*, the smaller aldehyde substituent at position *R1* may be less susceptible to protein structural changes and to inducing conformational distortion of the Chl macrocycle.

The Gaussian deconvolutions of the Chl solution spectra in the Q_y region (Fig. 3) serve as guides in the analysis of the absorption spectra of the reconstituted PCP complexes. Comparing the spectrum in the Q_y region of the Chl *a*-reconstituted PCP (Fig. 4A) with that of Chl *a* in solution (Fig. 3A) shows that two distinct pairs of Chl *a* Gaussian functions built on a broad background are needed to reproduce the spectrum of that complex. Likewise, for the PCP complex containing Chl *b*, two pairs of Gaussian components having different prominent spectral peaks and zero-phonon lines built on a broad background were needed to reproduce the spectrum of the protein complex (Fig. 4B). However, for the PCP complexes containing Chl *d* or 3-acetyl-Chl *a*, only two Gaussian components on a broad background were required to fit the spectra in the Q_y band region indicating that Chl *d* and 3-acetyl-Chl *a* in these complexes are in highly symmetric environments. This conclusion is supported by the observation that the PCP complexes reconstituted with Chl *a* and Chl *b* show a splitting in the Soret band region (Fig. 5A, B), but all the other complexes do not. This indicates a less symmetric environment for the Chls bound in the complexes containing Chl *a* or *b*.

The observation that the spectra of the PCP complexes containing Chl *a* and Chl *b* show splittings in the Soret and Q_y regions attributable to environmental asymmetry, but the spectra from the Chls in the other complexes do not, may also be traceable to the different functional groups on Ring I of the Chls. A view of the published structure of the MFPCP complex focusing on Chl 601 in the vicinity of Ring I shows that this part of the Chl macrocycle is in close proximity (within 4 Å) to peridinin 612 and 614 (Fig. 8). The distance between the vinyl group and the peridinin is closer than to any amino acid residue in the protein. Leucine-204 comes closest at ~5 Å (Fig. 8). The splitting of the Soret and Q_y spectral bands in the Chl *a* and Chl *b* PCP complexes implies that the vinyl group on Chl *a* and Chl *b* may adopt different configurations leading to distinct interactions between these Chls and

the peridinin. In contrast, the carbonyl groups on Ring I of Chl *d*, 3-acetyl-Chl *a* and BChl *a* may have only a single configuration and may also sterically hinder the approach of peridinin 612 and 614 toward the Chl in those complexes, thereby minimizing the interaction between pigments, rendering the Chl spectra equivalent.

The results from the deconvolution of the spectral features for the PCP complex containing BChl *a* are unusual. In addition to the main Q_y absorption band at 782 nm (Figs. 2, 4E), a shoulder at 799 nm is observed which is highly reminiscent of the 4 K absorption spectrum of the antenna BChl *a*-protein (Fenna-Matthews-Olson, FMO) complex from *Prosthecochloris aestuarii* (Johnson and Small 1991; Wendling et al. 2002; Whitten et al. 1978). The spectral features in the Q_y region are attributed to a combination of site shifts and dipolar interactions among the seven BChl *a* molecules within one subunit of the FMO protein (Wendling et al. 2002). The crystal structure of this FMO complex has been determined to 2.8 Å resolution (Matthews et al. 1979) and later refined to 1.9 Å resolution (Tronrud et al. 1986). The FMO complex consists of three identical subunits and each subunit contains seven BChl *a* molecules where the center-to-center distances between

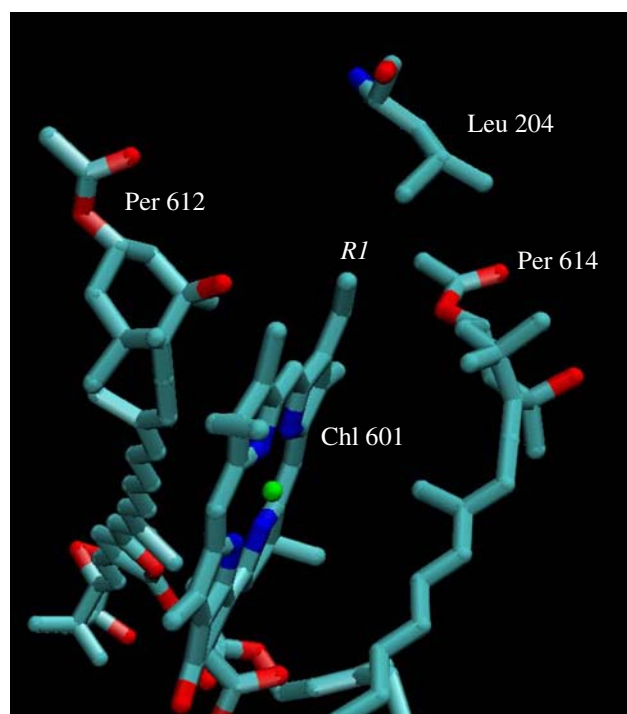


Fig. 8 A view of the structure of the MFPCP complex focusing on the Ring I of Chl 601. Per 612, Per 614 and Leu 204 are in close proximity to the Ring I of Chl 601. The coordinates of the structure were taken from Protein Data Bank with 1PPR code

BChls vary from 11 to 14 Å (Matthews et al. 1979). This is smaller than the center-to-center distance of 17.4 Å reported from the X-ray crystallographic analysis of the MFPCP complex containing Chl *a* (Hofmann et al. 1996). Why the BChl-containing complexes exhibit this long-wavelength feature in their spectra but the complexes containing the other Chl molecules do not, is unclear. Nevertheless, the Soret band and the Q_y features of the BChl molecules in the PCP complex are reproduced (Figs. 4E, 5E) assuming only a single prominent feature and a phonon line. Thus, similar to the complexes containing Chl *d* or 3-acetyl-Chl *a*, this suggests a highly symmetric environment for the BChls bound in this reconstituted PCP complex.

The Chl–protein interaction induces a blue-shift of the Q_y band in the low temperature spectra of Chl *a*, Chl *b* and 3-acetyl-Chl *a*, no shift for Chl *d*, and a red-shift for BChl *a* compared to the spectra taken in 2-MTHF low temperature glasses (Figs. 3, 4). This may be explained in a manner similar to that used above to interpret the blue-shifts of the Q_y bands induced upon lowering the temperature. Switching from a 2-MTHF glass to the protein may induce a conformational change of the macrocycle that leads to the observed shifts (Gudowska-Nowak et al. 1990). Structural differences between Chl species occur due to different functional groups attached at positions *R1* and *R2* (Fig. 1), but again, it appears that the *R1* site is key. The small aldehyde group of Chl *d* does not provide sufficient interaction leading to distortion of the macrocycle either in 2-MTHF glass or in the protein. Thus, essentially no protein-induced shift is observed. In contrast, the vinyl group on Ring I of Chl *a* and Chl *b* respond to the protein environment and induce a structural change that is manifested spectroscopically as a blue-shift of the Q_y band. The red-shift of BChl *a* in the protein can be attributed to the acetyl group in the position *R1*. This functional group has been shown to cause a substantial red-shift of absorption spectra of BChl *a* in LH2 complexes from photosynthetic bacteria (Cogdell et al. 2002). The rotation of the carbonyl group with respect to the plane of Ring I causes changes in π -electron conjugation and this argument has been used to interpret the difference between the B820 and B850 absorbing BChls in different LH2 complexes (Cogdell et al. 2002). However, if this were the sole effect, a protein-induced red-shift would be expected of the 3-acetyl-Chl *a* that also has an acetyl group in the *R1* site. This is not observed. Thus, we must assume that the saturation of the $-C=C-$ bond in Ring II for BChl also plays a role in determining the direction of the shift.

Energy transfer efficiencies

Light absorption by peridinin promotes the molecule from its ground state, S_0 , to an excited state, denoted S_2 . The S_2 state of peridinin then decays in ~ 100 fs to a lower-lying S_1 state which cannot be directly accessed from S_0 due to symmetry selection rules (Akimoto et al. 1996; Krueger et al. 2001; Zigmantas et al. 2003). Since the lifetime of the S_1 state of peridinin in solution was found to be highly dependent on the polarity of the solvent (Bautista et al. 1999; Zigmantas et al. 2001; 2003), an intramolecular charge transfer (ICT) state was invoked to account for this behavior (Bautista et al. 1999), and quantum computations have supported this model (Vaswani et al. 2003). Moreover, it has been argued from pump-dump-probe experiments on peridinin in solution that S_1 and ICT states are distinct but connected on a picosecond time-scale (Papagiannakis et al. 2004). However, other time-resolved and two-photon spectroscopic methods have suggested that it is the S_1 itself that possesses the charge transfer character (Shima et al. 2003; Zigmantas et al. 2003). Since it is not completely resolved whether the S_1 state in PCP is distinct from or the same as the ICT state, we shall use the notation S_1 /ICT to indicate both possibilities.

The peridinin-to-Chl energy transfer efficiencies for the complexes can be computed assuming a two-state (S_2 and S_1 /ICT) donor model (Fig. 9). The overall efficiency, ϵ , is given by Desamero et al. 1998:

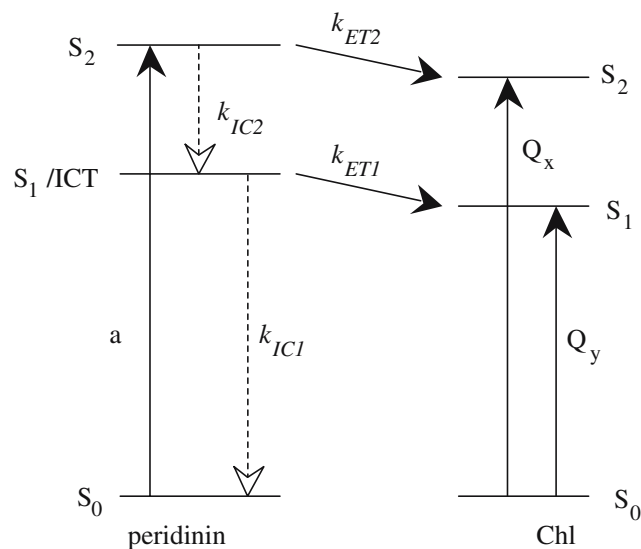


Fig. 9 Schematic diagram of energy levels and energy transfer pathways between peridinin and Chl in the PCP complexes. k_{ET1} and k_{ET2} (solid lines) are rate constants for energy transfer from the S_2 and S_1 /ICT states of peridinin to Chl. k_{IC2} and k_{IC1} (dashed lines) are rate constants for internal conversion from S_2 to S_1 /ICT and S_1 /ICT to S_0 , respectively

Table 2 Rate constants and energy transfer efficiencies obtained from the ultrafast, time-resolved optical spectroscopic experiments on the PCP complexes reconstituted with various Chls

PCP complex	k_{ET2} (ps ⁻¹)	k_{IC2} (ps ⁻¹)	k_{ET1} (ps ⁻¹)	k_{IC1} (ps ⁻¹)	ϵ (from fluorescence excitation), %	ϵ (from time-resolved absorption), %
Chl <i>a</i>	10 ± 2.5	15 ± 1.5	0.34 ± 0.034	0.063	94 ± 2	91 ± 7
Chl <i>b</i>	10 ± 2.5	15 ± 1.5	0.17 ± 0.017	0.063	92 ± 2	84 ± 14
Chl <i>d</i>	13 ± 3.0	15 ± 1.5	0.59 ± 0.059	0.063	96 ± 3	95 ± 2
aChl <i>a</i>	11 ± 2.8	15 ± 1.5	0.45 ± 0.045	0.063	99 ± 1	93 ± 4
BChl <i>a</i>	10 ± 2.5	15 ± 1.5	2.22 ± 0.22	0.063	~100	98 ± 2

k_{ET2} and k_{ET1} are the rate constants for energy transfer from the S₂ and S₁/ICT states of peridinin (Polívka et al 2005). k_{IC2} and k_{IC1} are the rate constants for internal conversion from S₂ to S₁/ICT and from S₁/ICT to S₀, respectively. k_{IC2} was obtained from fluorescence up-conversion measurement on the native PCP complex (Linden et al 2004). k_{IC1} was deduced from the efficiency and dynamics of energy transfer in the native MFPCP given in Ref. (Zigmantas et al 2002). k_{IC2} and k_{IC1} were assumed to be unchanged in all the PCP complexes. The peridinin-to-Chl energy transfer efficiency, ϵ , was obtained from steady-state fluorescence excitation experiments and from ultrafast, time-resolved absorption spectroscopic measurements at room temperature. The uncertainties in the values of ϵ from fluorescence excitation experiments were derived from the standard deviations obtained in the 450–515 nm wavelength range. The uncertainties in the values of ϵ from time-resolved absorption measurements were obtained by propagating the published errors in the dynamics

aChl *a* 3-acetyl-Chl *a*

$$\epsilon = \frac{k_{ET2}}{k_{ET2} + k_{IC2}} + \left[\frac{k_{IC2}}{k_{ET2} + k_{IC2}} \right] \left[\frac{k_{ET1}}{k_{ET1} + k_{IC1}} \right] \quad (1)$$

where k_{ET2} and k_{ET1} are the rate constants for energy transfer from the S₂ and S₁/ICT states of peridinin, k_{IC2} is the rate constant for internal conversion from S₂ to S₁/ICT state and k_{IC1} is the rate constant for S₁/ICT to S₀ internal conversion. The rate constants obtained directly from the ultrafast, time-resolved optical spectroscopic experiments carried out (Polívka et al. 2005) are shown in Table 2. The value for the rate constant for S₂ to S₁/ICT internal conversion, k_{IC2} , is assumed to be 15 ± 1.5 ps⁻¹ (τ_{IC2} = 66 ± 6 fs) from fluorescence up-conversion measurement on the native PCP complex (Linden et al. 2004). The value for k_{IC1} is assumed to be 0.063 ps⁻¹ (τ_{IC1} = 16 ps) from a measurement of the efficiency and dynamics of energy transfer in the native PCP complex (Zigmantas et al. 2003). The overall energy transfer efficiencies calculated from Eq. 1 are compared with the values obtained here from the steady-state measurements (Fig. 7) and summarized in Table 2. As one can see from the table, the efficiencies determined using both techniques are high in all cases and also in very reasonable agreement with each other.

In this work, it was shown that optical spectroscopy carried out at low temperatures provides a more highly resolved view of the spectral features of light-harvesting complexes than seen at room temperature. The steady-state optical spectroscopic methods applied to PCP complexes in which recombinant apoprotein has been refolded in the presence of peridinin and either Chl *a*, Chl *b*, Chl *d*, 3-acetyl-Chl *a* or BChl *a* illustrate the robust character of the PCP protein which maintains high efficiency of peridinin-to-chlorophyll

energy transfer function in the presence of non-native Chl species. The efficiencies of energy transfer deduced from the steady-state measurements are in good agreement with those from ultrafast, time-resolved experiments. The PCP complex continues to be an effective tool for elucidating the molecular details of photosynthetic light-harvesting via systematic modification of its structural components.

Acknowledgments This research is supported in the laboratory of HAF by the National Institutes of Health (GM-30353), and the University of Connecticut Research Foundation. RGH was supported by a Macquarie University research development grant. TP thanks the Swedish Energy Agency for financial support. Funding for TWC was provided by an NSF Research Experience for Undergraduates program (CHE-0354012) at the University of Connecticut.

References

- Akahane J, Fiedor L, Rondonuwu FS, Watanabe Y, Koyama Y (2004) Reconstitution of the LH1 antenna complex from *Rhodospirillum rubrum* G9 and wild type by the use of five carotenoids having different conjugation lengths. *Plant Cell Physiol* 45:S100
- Akimoto S, Takaichi S, Ogata T, Nishimura Y, Yamazaki I, Mimuro M (1996) Excitation energy transfer in carotenoid-chlorophyll protein complexes probed by femtosecond fluorescence decays. *Chem Phys Lett* 260:147–152
- Bautista JA, Connors RE, Raju BB, Hiller RG, Sharples FP, Gosztola D, Wasielewski MR, Frank HA (1999) Excited state properties of peridinin: observation of a solvent dependence of the lowest excited singlet state lifetime and spectral behavior unique among carotenoids. *J Phys Chem B* 103:8751–8758
- Bautista JA, Hiller RG, Sharples FP, Gosztola D, Wasielewski M, Frank HA (1999) Singlet and triplet energy transfer in the peridinin-chlorophyll *a*-protein from *Amphidinium carterae*. *J Phys Chem A* 103:2267–2273

- Cammarata KV, Plumley FG, Schmidt GF (1990) Reconstitution of light-harvesting complexes: a single apoprotein binds Chl *a*, Chl *b*, and xanthophylls. In: Baltscheffsky M (eds) Current research in photosynthesis, vol. 2. Kluwer Academic Publishers, Dordrecht, The Netherlands, pp. 341–344
- Carbonera D, Giacometti G, Segre U, Angerhofer A, Gross U (1999) Model for triplet-triplet energy transfer in natural clusters of peridinin molecules contained in Dinoflagellate's outer antenna proteins. *J Phys Chem B* 103:6357–6362
- Chadwick BW, Zhang C, Cogdell RJ, Frank HA (1987) The effects of lithium dodecyl sulfate and sodium borohydride on the absorption spectrum of the B800–850 light-harvesting complex from *Rhodospseudomonas acidophila* 7750. *Biochim Biophys Acta* 893:444–451
- Cogdell RJ, Howard TD, Isaacs NW, McLuskey K, Gardiner AT (2002) Structural factors which control the position of the Q_y absorption band of bacteriochlorophyll *a* in purple bacterial antenna complexes. *Photosynth Res* 74:135–141
- Crielaard W, Visschers RW, Fowler GJS, van Grondelle R, Hellingwerf KJ, Hunter CN (1994) Probing the B800 bacteriochlorophyll binding site of the accessory light-harvesting complex from *Rhodobacter sphaeroides* using site-directed mutants. I. Mutagenesis, effects on binding, function and electrochromic behaviour of its carotenoids. *Biochim Biophys Acta* 1183:473–482
- Croce R, Remelli R, Varotto C, Breton J, Bassi R (1999) The neoxanthin binding site of the major light harvesting complex (LHCII) from higher plants. *FEBS Lett* 456:1–6
- Damjanovic A, Ritz T, Schulten K (2000) Excitation transfer in the peridinin-chlorophyll-protein of *Amphidinium carterae*. *Biophys J* 79:1695–1705
- Davidson E, Cogdell RJ (1981) Reconstitution of carotenoids into the light-harvesting pigment-protein complex from the carotenoidless mutant of *Rhodospseudomonas sphaeroides* R26. *Biochim Biophys Acta* 635:295–303
- Desamero RZB, Chynwat V, van der Hoef I, Jansen FJ, Lugtenburg J, Gosztola D, Wasielewski MR, Cua A, Bocian DF, Frank HA (1998) The mechanism of energy transfer from carotenoids to bacteriochlorophyll: light-harvesting by carotenoids having different extents of *p*-electron conjugation incorporated into the B850 antenna complex from the carotenoidless bacterium *Rhodobacter sphaeroides* R-26.1. *J Phys Chem* 102:8151–8162
- Frank HA (1999) Incorporation of carotenoids into reaction center and light-harvesting pigment-protein complexes. In: Frank HA, Young AJ, Britton G, Cogdell RJ (eds) The photochemistry of carotenoids, vol. 8. Kluwer Academic Publishing, Dordrecht, The Netherlands, pp 235–244
- Fraser NJ, Dominy PJ, Ucker B, Simonin I, Scheer H, Cogdell RJ (1999) Selective release, removal, and reconstitution of bacteriochlorophyll *a* molecules into the B800 sites of LH2 complexes from *Rhodospseudomonas acidophila* 10050. *Biochemistry* 38:9684–9692
- Frigaard NU, Maresca JA, Yunker CE, Jones AD, Bryant DA (2004) Genetic manipulation of carotenoid biosynthesis in the green sulfur bacterium *Chlorobium tepidum*. *J Bacteriol* 186:5210–5220
- Germeroth L, Lottspeich F, Robert B, Michel H (1993) Unexpected similarities of the B800–850 light-harvesting complex from *Rhodospirillum rubrum* to the B870 light-harvesting complexes from other purple photosynthetic bacteria. *Biochemistry* 32:5615–5621
- Gudowska-Nowak E, Newton MD, Fajer J (1990) Conformational and environmental effects on bacteriochlorophyll optical spectra: correlations of calculated spectra with structural results. *J Phys Chem* 94:5795–5801
- Hofmann E, Wrench PM, Sharples FP, Hiller RG, Welte W, Diederichs K (1996) Structural basis of light harvesting by carotenoids: peridinin-chlorophyll-protein from *Amphidinium carterae*. *Science* 272:1788–1791
- Hu X, Xu D, Hamer K, Schulten K, Koepke J, Michel H (1995) Predicting the structure of the light-harvesting complex of *Rhodospirillum rubrum*. *Protein Sci* 4:1670–1682
- Ilagan RP, Shima S, Melkozernov A, Lin S, Blankenship RE, Sharples FP, Hiller RG, Birge RR, Frank HA (2004) Spectroscopic properties of the main-form and high-salt peridinin-chlorophyll *a*-proteins from *Amphidinium carterae*. *Biochemistry* 43:1478–1487
- Johnson SG, Small GJ (1991) Excited-state structure and energy-transfer dynamics of the bacteriochlorophyll *a* antenna complex from *Prosthecochloris aestuarii*. *J Phys Chem* 95:471–479
- Kleima FJ, Hofmann E, Gobets B, Van Stokkum IHM, Van Grondelle R, Diederichs K, Van Amerongen H (2000) Förster excitation energy transfer in peridinin-chlorophyll-*a*-protein. *Biophys J* 78:344–353
- Kleima FJ, Wendling M, Hofmann E, Peterman EJG, van Grondelle R, van Amerongen H (2000) Peridinin chlorophyll *a* protein: relating structure and steady-state spectroscopy. *Biochemistry* 39:5184–5195
- Koepke J, Hu X, Schulten K, Michel H (1996) The crystal structure of the light harvesting complex II (B800–850) from *Rhodospirillum rubrum*. *Structure* 4:581–597
- Krueger BP, Lampoura SS, van Stokkum IHM, Papagiannakis E, Salverda JM, Gradinaru CC, Rutkauskas D, Hiller RG, van Grondelle R (2001) Energy transfer in the peridinin chlorophyll *a* protein of *Amphidinium carterae* studied by polarized transient absorption and target analysis. *Biophys J* 80:2843–2855
- Kühlbrandt W, Wang DN, Fujiyoshi Y (1994) Atomic model of plant light-harvesting complex by electron crystallography. *Nature* 367:614–621
- Law CJ, Roszak AW, Southall J, Gardiner AT, Isaacs NW, Cogdell RJ (2004) The structure and function of bacterial light-harvesting complexes (Review). *Mol Membr Biol* 21:183–191
- Linden PA, Zimmermann J, Brixner T, Holt NE, Vaswani HM, Hiller RG, Fleming GR (2004) Transient absorption study of peridinin and peridinin chlorophyll *a* protein after two-photon excitation. *J Phys Chem B* 108:10340–10345
- Liu ZF, Yan HC, Wang KB, Kuang TY, Zhang JP, Gui LL, An XM, Chang WR (2004) Crystal structure of spinach major light-harvesting complex at 2.72 Å resolution. *Nature* 428:287–292
- Matthews BW, Fenna RE, Bolognesi MC, Schmid MF, Olson JM (1979) Structure of a bacteriochlorophyll *a*-protein from the green photosynthetic bacterium *Prosthecochloris aestuarii*. *J Mol Biol* 131:259–285
- McDermott G, Prince SM, Freer AA, Hawthornthwaite-Lawless AM, Papiz MZ, Cogdell RJ, Isaacs NW (1995) Crystal structure of an integral membrane light-harvesting complex from photosynthetic bacteria. *Nature* 374:517–521
- Miller DJ, Catmull J, Puskeiler R, Tweedale H, Sharples FP, Hiller RG (2005) Reconstitution of the peridinin chlorophyll *a* protein (PCP): evidence for functional flexibility in chlorophyll binding. *Photosynth Res* 86:229–240
- Morosinotto T, Castelletti S, Breton J, Bassi R, Croce R (2002) Mutation analysis of Lhc1 antenna complex. *J Biol Chem* 277:36253–36261
- Olivera LO, Westerhuis WHJ, Niederman RA (1994) Spectral alteration in *Rhodobacter capsulatus* mutants with site-directed changes in the bacteriochlorophyll-binding site of the B880 light-harvesting complex. *Biochim Biophys Acta* 1185:318–326

- Olsen JD, Sturgis JN, Westerhuis WHJ, Fowler GJS, Hunter CN, Robert N (1997) Site-directed modification of the ligands to the bacteriochlorophylls of the light-harvesting LH1 and LH2 complexes of *Rhodobacter sphaeroides*. *Biochemistry* 36:12625–12632
- Papagiannakis E, Larsen DS, van Stokkum IHM, Vengris M, Hiller RG, van Grondelle R (2004) Resolving the excited state equilibrium of peridinin in solution. *Biochemistry* 43:15303–15309
- Plumley FG, Schmidt GW (1987) Reconstitution of chlorophyll *a/b* light-harvesting complexes: xanthophyll-dependent assembly and energy transfer. *Proc Natl Acad Sci USA* 83:146–150
- Polívka T, Pascher T, Sundström V, Hiller RG (2005) Tuning energy transfer in the peridinin–chlorophyll complex by reconstitution with different chlorophylls. *Photosynth Res* 86:217–227
- Remelli R, Varotto C, Sandona D, Croce R, Bassi R (1999) Chlorophyll binding to monomeric light-harvesting complex. *J Biol Chem* 274:33510–33521
- Ritz T, Damjanovic A, Schulten K, Zhang J-P, Koyama Y (2000) Efficient light harvesting through carotenoids. *Photosynth Res* 66:125–144
- Roszak AW, Howard TD, Southall J, Gardiner AT, Law CJ, Isaacs NW, Cogdell RJ (2003) Crystal structure of the RC-LH1 core complex from *Rhodospseudomonas palustris*. *Science* 302:1969–1972
- Sharples FP, Wrench PM, Ou K, Hiller RG (1996) Two distinct forms of the peridinin-chlorophyll *a*-protein from *Amphidinium carterae*. *Biochim Biophys Acta* 1276:117–123
- Shima S, Ilagan RP, Gillespie N, Sommer BJ, Hiller RG, Sharples FP, Frank HA, Birge RR (2003) Two-photon and fluorescence spectroscopy and the effect of environment on the photochemical properties of peridinin in solution and in the peridinin-chlorophyll-protein from *Amphidinium carterae*. *J Phys Chem A* 107:8052–8066
- Struck A, Müller A, Scheer H (1991) Modified bacterial reaction centers: 4: the borohydride treatment reinvestigated. Comparison with selective exchange experiments at binding sites B_{A,B} and H_{A,B}. *Biochim Biophys Acta* 1060:262–270
- Struck A, Cmiel E, Katheder I, Schäfer W, Scheer H (1992) Bacteriochlorophylls modified at position C-3; long-range intramolecular interaction with position C-13². *Biochim Biophys Acta* 1101:321–328
- Tronrud DE, Schmid MF, Matthews BW (1986) Structure and X-ray amino acid sequence of a bacteriochlorophyll *a* protein from *Prosthecochloris aestuarii* refined at 1.9 Å resolution. *J Mol Biol* 188:443–454
- Vaswani HM, Hsu CP, Head-Gordon M, Fleming GR (2003) Quantum chemical evidence for an intramolecular charge-transfer state in the carotenoid peridinin of peridinin-chlorophyll-protein. *J Phys Chem B* 107:7940–7946
- Wendling M, Przyjalowski MA, Gulen D, Vulto SIE, Aartsma TJ, van Grondelle R, van Amerongen H (2002) The quantitative relationship between the structure and polarized spectroscopy in the FMO complex of *Prosthecochloris aestuarii*: refining experiments and simulations. *Photosynth Res* 71:99–123
- Whitten WB, Nairn JA, Pearlstein RM (1978) Derivative absorption spectroscopy from 5–300 K of bacteriochlorophyll *a*-protein from *Prosthecochloris aestuarii*. *Biochim Biophys Acta* 503:251–262
- Wu HM, Ratsep M, Jankowiak R, Cogdell RJ, Small GJ (1997) Comparison of the LH2 antenna complexes of *Rhodospseudomonas acidophila* (strain 10050) and *Rhodobacter sphaeroides* by high-pressure absorption, high-pressure hole burning, and temperature-dependent absorption spectroscopies. *J Phys Chem B* 101:7641–7653
- Zigmantas D, Polívka T, Hiller RG, Yartsev A, Sundström V (2001) Spectroscopic and dynamic properties of the peridinin lowest singlet excited states. *J Phys Chem A* 105:10296–10306
- Zigmantas D, Hiller RG, Polívka T, Sundström V (2002) Carotenoid to chlorophyll energy transfer in the peridinin chlorophyll-*a*-protein complex: a unique pathway involving an intramolecular charge transfer state. *Proc Natl Acad Sci USA* 99:16760–16765
- Zigmantas D, Hiller RG, Yartsev A, Sundström V, Polívka T (2003) Dynamics of excited states of the carotenoid peridinin in polar solvents: dependence on excitation wavelength, viscosity, and temperature. *J Phys Chem B* 107:5339–5348
- Zimmermann J, Linden PA, Vaswani HM, Hiller RG, Fleming GR (2002) Two-photon excitation study of peridinin in benzene and in the peridinin-chlorophyll *a*-protein (PCP). *J Phys Chem B* 106:9418–9423